Modelling small and large displacements of a sphere on an elastic half-space exposed to a dynamic force

This is a post-refereeing final draft. When citing, please refer to the published version: Hasan Koruk (2021), Modelling small and large displacements of a sphere on an elastic half-space exposed to a dynamic force , *European Journal of Physics, 42 (5), 055006*, DOI: 10.1088/1361-6404/ac0e42 . https://doi.org/10.1088/1361-6404/ac0e42

Modelling small and large displacements of a sphere on an elastic half-space exposed to a dynamic force

H Koruk[1]
[1]Mechanical Engineering Department, MEF University, 34396 Istanbul, Turkey

Tel.: +902123953654. Email: korukh@mef.edu.tr

Abstract

Spheres at medium interfaces are encountered in many applications, including in atomic force microscopy or indentation tests. Although the Hertz theory describes the contact mechanics between an elastic sphere and an elastic half-space for static loading and small deformations very well, there is a need to consider the density of the medium, the mass of the sphere and the radiation damping for dynamic loading to obtain reliable results. In this study, an analytical model for predicting the small and large displacements of a sphere on an elastic half-space exposed to a dynamic force is developed. For this purpose, after summarizing a mathematical model that has recently been proposed for the sphere at a medium interface, a finite element model for the sphere at an elastic interface is developed. Based on the comparison of the mathematical and finite element models, an improved analytical model for the sphere at an elastic interface is developed. In addition to considering the elastic properties of the medium and the size of the sphere, the model developed here takes into account the density of the medium, the mass of the sphere, and the radiation damping, and the model is valid for small and large sphere displacements. The developed model can be used to understand the dynamic responses of spherical objects at medium interfaces in practical applications. Furthermore, the proposed model is a remarkable tool for undergraduate and graduate students and researchers in the fields of engineering, materials science and physics to gain insight into the dynamic responses of spheres at medium interfaces.

Keywords: elastic half space, interface, sphere, small oscillation, large oscillation, finite element model, Hertz model

1. Introduction

Spheres at medium interfaces are encountered in many applications, including in atomic force microscopy or indentation tests [1–5]. Although the Hertz theory can describe the contact mechanics between an elastic sphere and an elastic half-space for static loading and small deformations very well [6,7], there is a need to consider the density of the medium, the mass of the sphere and the radiation damping for dynamic loading to obtain reliable results. Although some studies have been performed to investigate the small [8] and nonlinear [9] oscillations of a sphere on an elastic half space, the effects of the density of the medium and the radiation damping has not been considered in these studies. A mathematical model has been proposed to predict the dynamic response of a sphere at a medium interface by taking into account the damping of the oscillations of the sphere due to the radiation of shear waves [10]. Although this model has recently been evaluated using the responses of the bubble and the sphere in a medium [11] and the bubble at a medium interface [12,13], and it has been noted that the model produces reasonable results [14], this model has not been validated using a reference model, such as a finite element model, or experimental data. In this study, a finite element model for the sphere at an elastic interface is developed and the performance of the mathematical model in [10] is evaluated using the finite element analysis results first time in the literature. Furthermore, based on the comparison of the mathematical model in [10] and the finite element model, an improved analytical model for the sphere at an elastic interface is developed.

In addition to considering the elastic properties of the medium and the size of the sphere, the model developed in this study takes into account the density of the medium, the mass of the sphere, and the radiation damping for dynamic loading, and the developed model is valid for small and large sphere displacements. Based on the results of the finite element model of the sphere at an elastic medium interface, accurate models for the force related to the system stiffness, the force component related to the damping of the oscillations of the sphere due to the radiation of shear waves and the inertia force due to the mass of the elastic medium involved in motion are obtained in this study for the first time in the literature. Furthermore, the dynamic response of a sphere at an elastic medium interface to a rectangular pulse with the amplitude of f_0 and a duration of τ (i.e., the constant force f_0 is applied for a short time τ and then removed) is determined in this study. It should be noted that the response to the rectangular pulse simulates the impulse response for small τ values and the step response for large τ values with $0 \leq t \leq \tau$. Therefore, the model presented in this study can be used to determine the correct amplitudes and frequency of oscillations and the correct steady-state displacement of the sphere at an elastic medium interface. It is believed that the model presented in this study is the most comprehensive dynamic Hertz model in the literature, because it includes accurate models for elastic force, radiation damping and the inertia force due the mass of the medium involved in motion. Furthermore, the procedure for obtaining a comprehensive and correct dynamic Hertz model in this study is a remarkable tool for undergraduate and graduate students and researchers in the fields of engineering, materials science and physics. The approach presented in this study can be used, especially, in post-

graduate engineering, material science and physics courses, to provide a procedure for the dynamic response analysis of a sphere at an elastic medium interface, by taking into account correct elastic force, radiation damping and inertia force due to the mass of the medium involved in motion.

The outline of the paper is as follows: First, the mathematical model proposed for the sphere at an elastic interface in [10] is summarized (Section 2.1). After that, a finite element model for the sphere at an elastic interface is developed (Section 2.2), and the performance of the analytical model is evaluated using the finite element model (Section 2.3). Then, based on the comparison of the analytical model and the finite element model, an improved analytical model for the sphere at an elastic interface is developed (Sections 3.1-3.5). Finally, the developed model is evaluated (Section 3.6) and some concluding remarks are given (Section 4). The proposed model can be used to understand the dynamic responses of spheres at medium interfaces in practical applications. Furthermore, the developed model can be a remarkable tool for undergraduate and graduate students in the fields of engineering, materials science and physics to understand the derivation of the equation of motion of the sphere at a medium interface by considering the radiation damping, to obtain an analytical solution for a damped system, and to use the finite element method to model the same problem.

2. Problem formulation

The schematic picture for the sphere at a medium interface is shown in figure 1. Here, the dynamic response of the sphere at an elastic medium interface with different shear moduli (650 Pa – 10 GPa) are investigated. It should be noted that the shear modulus of soft tissue such as the brain and liver and tissue-mimicking materials commonly used in practice such gelation is 200 – 2000 Pa [15–19]. On the other hand, traditional materials such as metals have a shear modulus of tens of GPa [20]. The procedure for obtaining an accurate analytical model for predicting the small and large displacements of a sphere on an elastic half-space exposed to a dynamic force is shown in figure 2. The derivation and evaluation of the model is presented in the following sections.

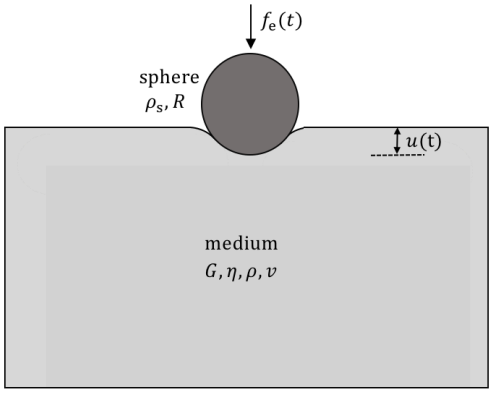

Figure 1. The schematic picture for the sphere at a medium interface.

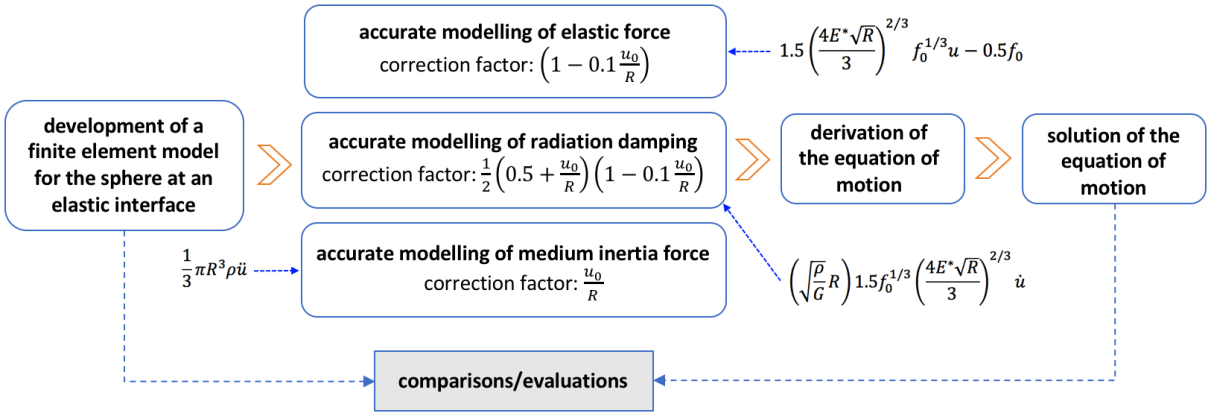

Figure 2. The procedure for obtaining an accurate analytical model for predicting the small and large displacements of a sphere on an elastic half-space exposed to a dynamic force.

2.1 Analytical model for the sphere at an elastic interface

A model for the analysis of the dynamic response of the sphere at a viscoelastic medium interface was proposed in [10]. It should be noted that the analytical solution of the model in [10] is not possible. By ignoring the medium viscosity (i.e., $\eta = 0$), the following model can be written for the dynamic response of the sphere at an elastic interface to a rectangular pulse:

$$u(t)=\frac{1}{2\pi}\int_{-\infty}^{\infty}\frac{(-jf_0/\omega)\left(e^{j\omega\tau}-1\right)e^{-j\omega t}}{-\frac{2}{9}\pi R^3(4\rho_s+\rho)\omega^2+f_0^{1/3}\left[\frac{8G(1+\nu)\sqrt{R}}{3(1-\nu^2)}\right]^{2/3}\left(1-\frac{1}{2}j\omega\sqrt{\frac{\rho}{G}}R\right)}\mathrm{d}\omega \tag{1}$$

where f_0 and τ are the amplitude and duration of the applied force, R and ρ_s are the radius and density of the sphere, G, ρ and ν are the shear modulus, density and Poisson's ratio of the elastic medium, t and ω show the time and frequency, respectively, and $j=\sqrt{-1}$. It should be noted that an improved analytical model for the dynamic response of the sphere at an elastic medium interface is presented below. The extension of this model to a sphere at a viscoelastic medium interface is considered as a future study.

2.2 Finite element model for the sphere at an elastic interface

The model in Eq. (1) has recently been evaluated using the responses of the bubble and the sphere in a medium [11] and the bubble at an interface [12,13], and it has been noted that the model produces reasonable results [14]. However, this model has not been validated using a reference model, such as a finite element model, or experimental data. Here, a finite element model for the sphere at an elastic interface is developed to assess the performance of the model presented in Eq. (1). As a three-dimensional model of the system requires a huge number of solid finite elements, a simplified finite element model of the system is developed using axisymmetric quadrilateral finite elements. For the finite element model of the sphere at a medium interface, the elastic medium is modelled using linear quadrilateral axisymmetric reduced integration elements of type CAX4R, and the sphere is modelled as a two-

dimensional analytical rigid shell in the Abaqus software (Dassault Systèmes, France). In addition, the sphere is modelled using linear line elements of type RAX2, and it is seen that almost the same results are obtained when 30 or more RAX2 elements for the sphere are used. The geometry is partitioned to able to use fine mesh around the sphere and coarser mesh far from the sphere. Linear elastic material for the medium, appropriate boundary conditions (no sphere displacement in horizontal direction), sphere-medium contact interaction (frictionless, hard contact) are defined and the model is run using the explicit dynamic analysis procedure. The finite element model for the sphere at an elastic medium interface is shown in figure 3.

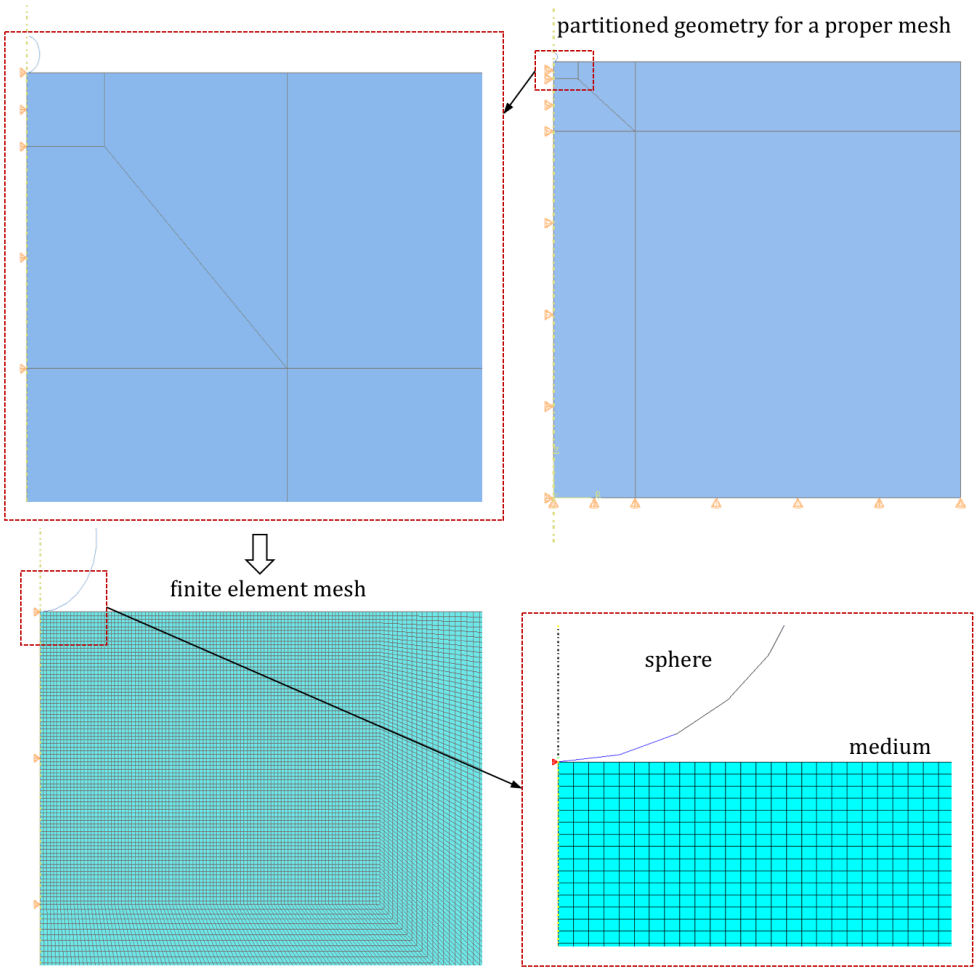

Figure 3. The finite element model for the sphere at an elastic medium interface.

In order to ensure that there are no reflections from the boundaries in the time duration of interest and to confirm the results, two different models are developed here. In the first model, a cylindrical medium of h = 50 mm height and r = 50 mm radius is modelled using 55000 CAX4R elements. In the second model, a cylindrical medium of h = 100 mm height and r = 100 mm radius is modelled using 130235 CAX4R elements. The displacements of the sphere at an elastic medium interface for both models are shown in figure 4. Here, the properties of the medium are $G = 650$ Pa, $\rho = 1000$ kg/m^3, $v = 0.45$, the radius and density of the sphere are $R = 0.5$ mm and ρ_s = 8000 kg/m^3, and the amplitude of force is $f_0 = 0.025$ mN. It is seen that both models produce the same results for t < 100 ms. Reflections

interfere with sphere displacements after around t = 100 and 200 ms for the first and second models, respectively.

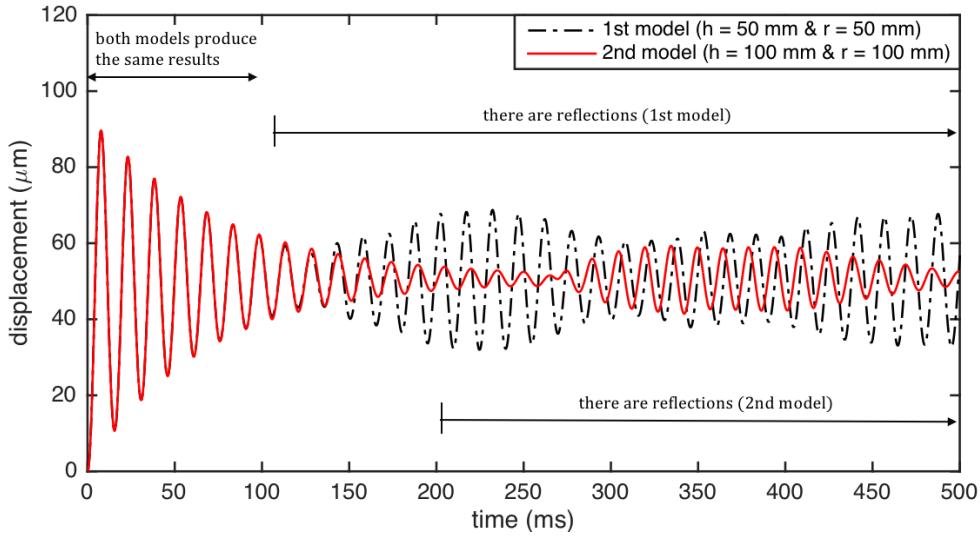

Figure 4. The displacements of the sphere at an elastic medium interface for both finite element models ($G = 650$ Pa, $\rho = 1000$ kg/m^3, $v = 0.45$, $R = 0.5$ mm, ρ_s = 8000 kg/m^3 and $f_0 = 0.025$ mN).

2.3 Evaluation of the analytical model for the sphere at an elastic medium interface

The displacements of the sphere at an elastic medium interface for different force levels precited by the analytical model (Eq. 1) and the finite element model are shown in figure 5. For the analytical model, the excitation duration τ was divided into N (e.g., 2000) points and the calculations were repeated over the entire time period of interest using the Matlab software (Mathworks, Natick, MA). Here, the properties of the medium are $G = 650$ Pa, $\rho = 1000$ kg/m^3, $v = 0.45$, and the radius and density of the sphere are $R = 0.5$ mm and ρ_s = 8000 kg/m^3, respectively. It is seen that the differences between the period (or frequency) of oscillations and the steady-state displacements predicted by the analytical and finite element models increase as the force magnitude (or the sphere displacement) increases. On the other hand, the differences between the amplitudes of oscillations precited by the analytical and finite element models are higher for lower force amplitudes (or lower sphere displacements). For example, the frequency of oscillations predicted by the analytical model is around 3% higher than the frequency of oscillations predicted by the finite element model, while the steady-state displacement predicted by the analytical model is around 4% lower than the steady-state displacement predicted by the finite element model for $f_0 = 40$ mN. These results show that the force related to the stiffness of the system becomes higher than the actual force when applied force (or sphere displacement) increases. Based on these results, an improved model for the sphere at an elastic medium interface is developed in the next section.

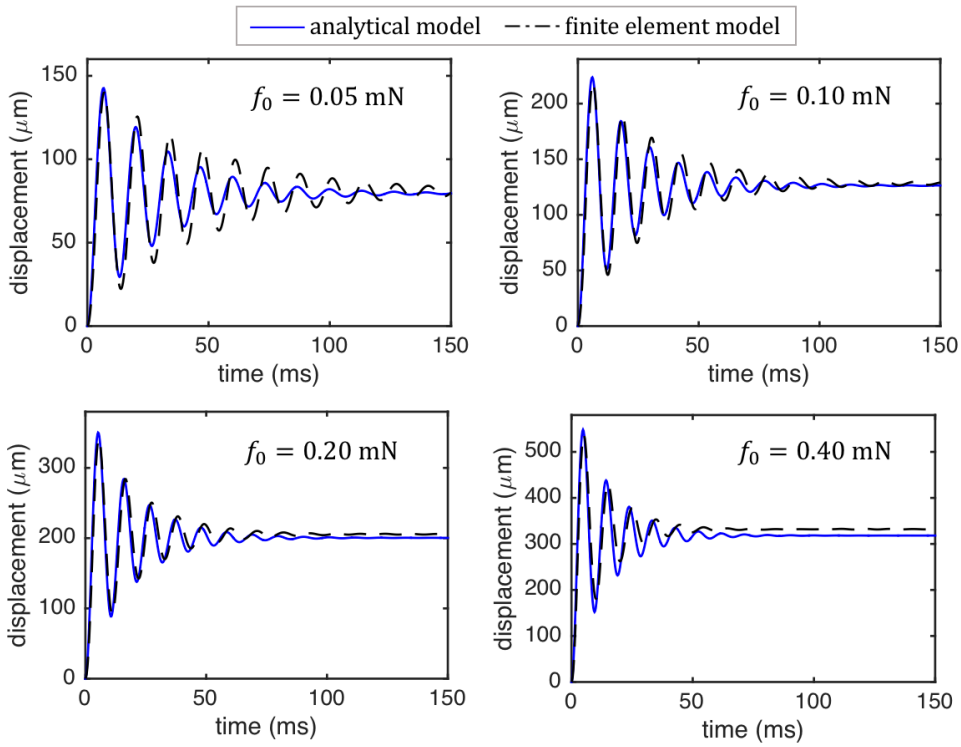

Figure 5. The displacements of the sphere at an elastic medium interface for different force levels precited by the analytical model (Eq. 1) and the finite element model ($G = 650$ Pa, $\rho = 1000$ kg/m^3, $v = 0.45$, $R = 0.5$ mm and $\rho_s = 8000$ kg/m^3).

3. An improved analytical model for the sphere at an elastic medium interface

The equation of motion of a sphere at an elastic interface can be written as:

$$f_e = f_i + f_s + f_r \tag{2}$$

where f_e is the external force applied to the sphere, f_i the inertia force, f_s is the force related to the system stiffness, and f_r shows the damping of the oscillations of the sphere due to the radiation of shear waves.

3.1 Correction for elastic force

The force related to the system stiffness is obtained from the Hertz contact theory, given by (Johnson, 1985):

$$f_0 = \frac{4E^*\sqrt{R^*}}{3} u_0^{3/2} \tag{3}$$

where f_0 is the applied force, R^* is the relative radius, and u_0 is the deformation of the surface from its initial position. Here, E^* is the reduced Young's modulus, computed as:

$$\frac{1}{E^*} = \frac{1-\nu_{\text{sphere}}^2}{E_{\text{sphere}}} + \frac{1-\nu^2}{E} \tag{4}$$

where ν_{sphere} and E_{sphere} are the Poisson's ratio and Young's modulus of the sphere, and ν and E are the Poisson's ratio and Young's modulus of the elastic medium, respectively. A linear relationship between force and displacement can be obtained by defining an equivalent stiffness coefficient [10] or using the Taylor's expansion [8]:

$$f_s \cong f(u_0) + \left.\frac{df}{du}\right|_{u_0} (u - u_0) = 1.5\frac{4E^*\sqrt{R^*}}{3} u_0^{1/2} u - 0.5\frac{4E^*\sqrt{R^*}}{3} u_0^{3/2} \tag{5}$$

Using the relationship in Eq. (3), Eq. (5) can be written as:

$$f_s = 1.5\left(\frac{4E^*\sqrt{R^*}}{3}\right)^{2/3} f_0^{1/3} u - 0.5 f_0 \tag{6}$$

It is shown in Section 2 that the expression in Eq. (6) used in [10] produces 3-4% errors in the frequency of oscillations and the steady-state displacement for $u_0 = R$. Therefore, the elastic force is revised so that it is decreased with sphere displacement in this study. A correction factor $\left(1 - a\frac{u_0}{R}\right)$ is used in this study for accurate description of the elastic force where a is a constant. This guarantees that the correction factor is zero when $u_0 = 0$ and decreases as sphere displacement increases. The amount of decrease (i.e., the value of a) is determined based on the finite element analysis results. Overall, the force related to the system stiffness is defined as follows:

$$f_s = \left(1 - a\frac{u_0}{R}\right)\left[1.5\left(\frac{4E^*\sqrt{R^*}}{3}\right)^{2/3} f_0^{1/3} u - 0.5 f_0\right] \tag{7}$$

It should be remembered that u_0 is given by $u_0 = \left(\frac{3f_0}{4E^*\sqrt{R^*}}\right)^{2/3}$. The force as a function of normalized steady-state displacement predicted by the finite element model, the model in [10] and the model proposed here for different a values are plotted in figure 6. It is seen that the force level for the model proposed here for $a = 0.05$ is greater than the one for the finite element model. The force level for the model proposed here for $a = 0.15$ is less than the one for the finite element model. On the other hand, the force level of the model proposed here for $a = 0.1$ is almost the same with the one for the finite element model. As shown in detail in Section 3.6, $a = 0.1$ produces very accurate results for different medium properties and force values. It should be noted that a correction of $a = 0.1$ corresponds to 10% decrease in force for $u_0 = R$.

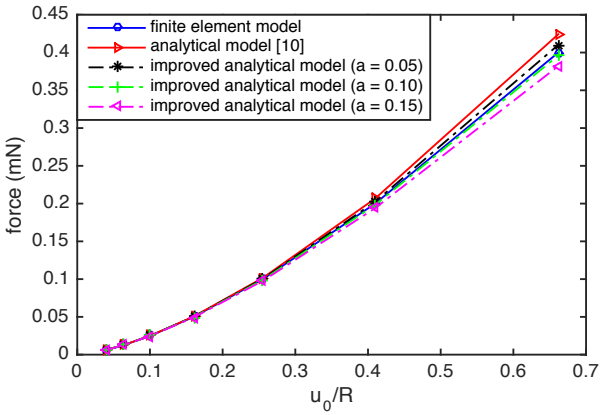

Figure 6. The force as a function of normalized steady-state displacement predicted by the finite element model, the model in [10] and the model proposed here for different a values ($G = 650$ Pa, $\rho = 1000$ kg/m^3, $v = 0.45$, $R = 0.5$ mm and ρ_s = 8000 kg/m^3).

3.2 Correction for radiation damping

The following expression derived for the force component related to the damping of the oscillations of the sphere due to the radiation of shear waves for the sphere at an elastic medium interface in [10]:

$$f_r = \frac{1}{2}\left(\sqrt{\frac{\rho}{G}}R\right)1.5f_0^{1/3}\left(\frac{4E^*\sqrt{R}}{3}\right)^{2/3}\dot{u} \tag{8}$$

where $\dot{u}$ is the velocity of the sphere, and G is the shear modulus of the elastic medium. In the model in [10], the force related to radiation damping is assumed to be constant (the value at $u_0 = R$ is used in the model). However, because more medium is involved in motion as sphere displacement increases, this force component should increase as sphere displacement increases. A correction factor $\left(b + \frac{u_0}{R}\right)$ is used in this study for accurate description of the radiation damping (where b is a constant) so that it guarantees that the correction factor is unity when $u_0 = R/2$ and increases as sphere displacement increases. Therefore, the radiation damping component is revised in this study as follows:

$$f_r = \frac{1}{2}\left(b + \frac{u_0}{R}\right)\left(\sqrt{\frac{\rho}{G}}R\right)\left(1 - a\frac{u_0}{R}\right)1.5f_0^{1/3}\left(\frac{4E^*\sqrt{R}}{3}\right)^{2/3}\dot{u} \tag{9}$$

The amplitudes of oscillations (here for the fifth peak) as a function of normalized steady-state displacement predicted by the finite element model, the model in [10] and the model proposed here for different b values are plotted in figure 7. As seen in figure 7 and as shown in detail in Section 3.6, $b = 0.5$ produces very accurate results for different medium properties and force values.

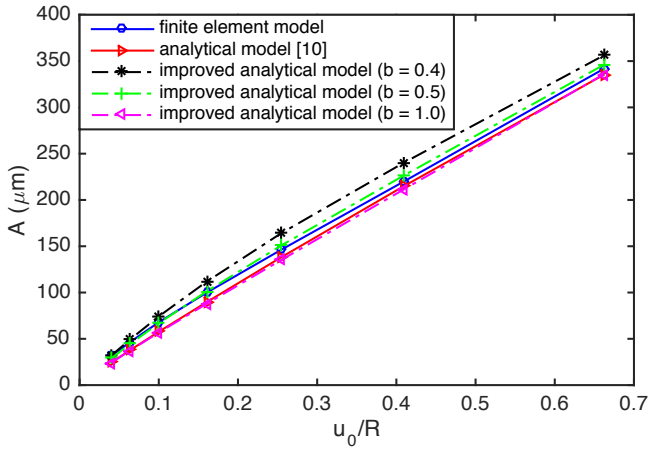

Figure 7. The amplitudes of oscillations (here for the fifth peak) as a function of normalized steady-state displacement predicted by the finite element model, the model in [10] and the model proposed here for different b values ($G = 650$ Pa, $\rho = 1000$ kg/m^3, $v = 0.45$, $R =$ 0.5 mm and ρ_s = 8000 kg/m^3).

3.3 Correction for inertia force

The inertia force due to the mass of the sphere is $f_{\text{i,sphere}} = \frac{4}{3}\pi R^3 \rho_s \ddot{u}$ where $\ddot{u}$ is the acceleration of the sphere. The inertia force due to the mass of the elastic medium involved in motion for the sphere in the medium is given as $f_{\text{i,medium}} = \frac{2}{3}\pi R^3 \rho \ddot{u}$ [11]. The inertia force due to the mass of the elastic medium involved in motion for the sphere at a medium interface was taken constant as $f_{\text{i,medium}} = \frac{1}{3}\pi R^3 \rho \ddot{u}$ [10]. As the inertia force due to the mass of the elastic medium involved in motion for the sphere at the medium interface would change from 0 for zero displacement to $\frac{2}{3}\pi R^3 \rho \ddot{u}$ for a displacement equal to $2R$, it is defined as $\frac{u_0}{2R}\frac{2}{3}\pi R^3 \rho \ddot{u} = \frac{u_0}{3R}\pi R^3 \rho \ddot{u}$ in this study. Hence, the inertia force becomes:

$$f_i = \frac{4}{3}\pi R^3 \rho_s \ddot{u} + \frac{u_0}{3R}\pi R^3 \rho \ddot{u} \tag{10}$$

3.4 Equation of motion

Using the force components derived in Section 3.3 and Eq. (2), the equation of motion for the sphere at an elastic medium interface can be written as follows:

$$\frac{4}{3}\pi R^3 \rho_s \ddot{u} + \frac{u_0}{3R}\pi R^3 \rho \ddot{u} + \frac{1}{2}\left(b + \frac{u_0}{R}\right)\left(\sqrt{\frac{\rho}{G}}R\right)\left(1 - a\frac{u_0}{R}\right)1.5 f_0^{1/3}\left(\frac{4E^*\sqrt{R}}{3}\right)^{2/3}\dot{u} +$$
$$\left(1 - a\frac{u_0}{R}\right)\left[1.5\left(\frac{4E^*\sqrt{R^*}}{3}\right)^{2/3} f_0^{1/3} u - 0.5 f_0\right] = f_e \tag{11}$$

Now, let's consider the external force as a rectangular pulse with the amplitude of f_0 and a duration of τ (i.e., the constant force f_0 is applied for a short time τ and then it is removed). For, $0 \leq t \leq \tau$, the equation of motion of the sphere at an elastic medium interface becomes:

$$\frac{1}{3}\pi R^3(4\rho_s + \rho)\ddot{u} + \frac{1}{2}\left(b + \frac{u_0}{R}\right)\left(\sqrt{\frac{\rho}{G}}R\right)\left(1 - a\frac{u_0}{R}\right)1.5f_0^{1/3}\left(\frac{4E^*\sqrt{R}}{3}\right)^{2/3}\dot{u} + \left(1 - a\frac{u_0}{R}\right)1.5\left(\frac{4E^*\sqrt{R^*}}{3}\right)^{2/3}f_0^{1/3}u = \left[1 + 0.5\left(1 - a\frac{u_0}{R}\right)\right]f_0 \quad (12)$$

3.5 Analytical solution

It is seen that Eq. (12) looks like a viscously damped system. Please note that the energy loss is because of the damping of the oscillations of the sphere due to the radiation of shear waves here. The solution of such a system can be written as [21]:

$$u(t) = \frac{f}{k} - \frac{f}{k\sqrt{1-\zeta^2}}e^{-\zeta\omega_n t}\cos(\omega_d t - \varphi) \qquad \text{for } 0 \leq t \leq \tau \quad (13a)$$

$$u(t) = \frac{fe^{-\zeta\omega_n t}}{k\sqrt{1-\zeta^2}}\left\{e^{\zeta\omega_n \tau}\cos[\omega_d(t-\tau) - \varphi] - \cos(\omega_d t - \varphi)\right\} \qquad \text{for } t > \tau \quad (13b)$$

Here, k is the equivalent stiffness coefficient, f is the effective force, ω_n is the undamped natural frequency, ω_d is the damped natural frequency, φ is the phase angle, ζ is the damping coefficient, m is the effective mass, c is effective damping coefficient, and c_{cr} is the critical damping coefficient given by:

$$k = \left(1 - a\frac{u_0}{R}\right)1.5\left(\frac{4E^*\sqrt{R^*}}{3}\right)^{2/3}f_0^{1/3} \quad (14)$$

$$c = \frac{1}{2}\left(b + \frac{u_0}{R}\right)\left(\sqrt{\frac{\rho}{G}}R\right)\left(1 - a\frac{u_0}{R}\right)1.5f_0^{1/3}\left(\frac{4E^*\sqrt{R}}{3}\right)^{2/3} \quad (15)$$

$$m = \frac{1}{3}\pi R^3(4\rho_s + \rho) \quad (16)$$

$$f = \left[1 + 0.5\left(1 - a\frac{u_0}{R}\right)\right]f_0 \quad (17)$$

$$\omega_n = \sqrt{\frac{k}{m}} \quad (18)$$

$$\omega_d = \omega_n\sqrt{1-\zeta^2} \quad (19)$$

$$\zeta = \frac{c}{c_{cr}} = \frac{c}{2\sqrt{km}} \quad (20)$$

$$\varphi = \tan^{-1}\frac{\zeta}{\sqrt{1-\zeta^2}} \tag{21}$$

The reduced Young's modulus becomes $E^* = E/(1-\nu^2)$ when the sphere is not deformable. The elasticity modulus is related to the shear modulus by $E = 2G(1+\nu)$ for homogeneous isotropic materials. Hence, we obtain $E^* = 2G(1+\nu)/(1-\nu^2)$ for a homogeneous isotropic material and a non-deformable sphere.

3.6 Evaluation of the improved analytical model

The displacements of the sphere at an elastic medium interface for different force levels precited by the improved analytical model (Eq. 13) and the finite element model using the same parameters in figure 5 are shown in figure 8. It is seen that, opposite to the original analytical model (figure 5), the results (i.e., the amplitudes and periods of oscillations and the steady-state displacements) predicted by the improved analytical model and the finite element model (figure 8) are almost the same. The amplitude of the displacement of the sphere precited by the improved analytical model and the finite element model decays almost with the same rate. This shows that the damping of the oscillations of the sphere due to the radiation of shear waves is properly described in the improved analytical model.

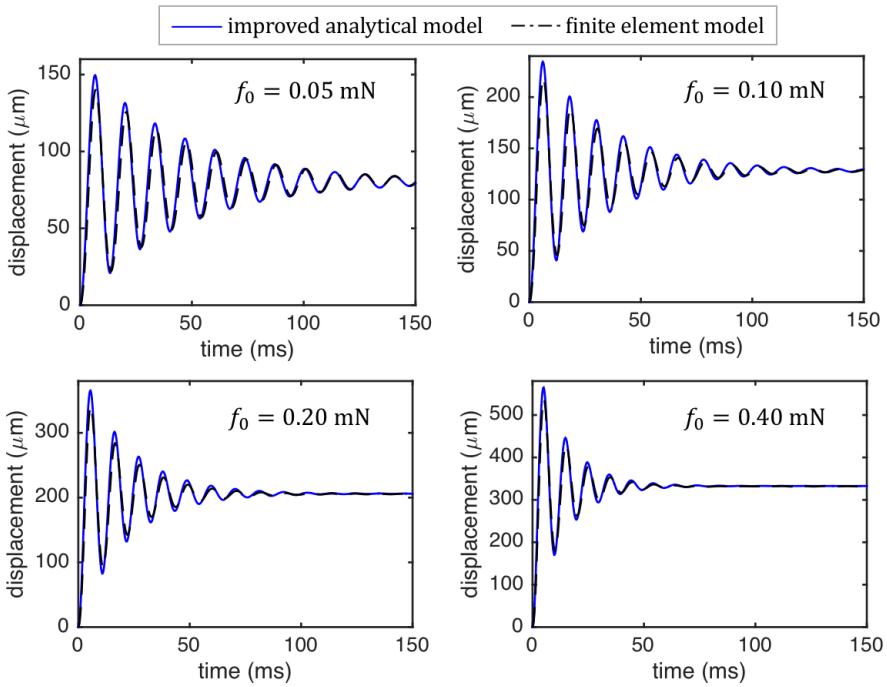

Figure 8. The displacements of the sphere at an elastic medium interface for different force levels precited by the improved analytical model (Eq. 13) and the finite element model ($G = 650$ Pa, $\rho = 1000$ kg/m^3, $\nu = 0.45$, $R = 0.5$ mm and ρ_s = 8000 kg/m^3).

The differences between (a) the amplitudes of oscillations (here for the fifth peak) and (b) the steady-state displacements predicted by the analytical model (Eq. 1) and the improved

analytical model developed in this study (Eq. 13) and the finite element model for different force levels or dimensionless displacements are plotted in figure 9 ($G = 650$ Pa, $\rho = 1000$ kg/m^3, $\nu = 0.45$, $R = 0.5$ mm and ρ_s = 8000 kg/m^3). It is clearly seen that, even for very high dimensionless sphere displacements (i.e., u_0/R), the improved analytical model produces very similar results with the finite element model (the differences are close to zero). On the other hand, the differences between the analytical model in [10] and the finite element model can be quite high.

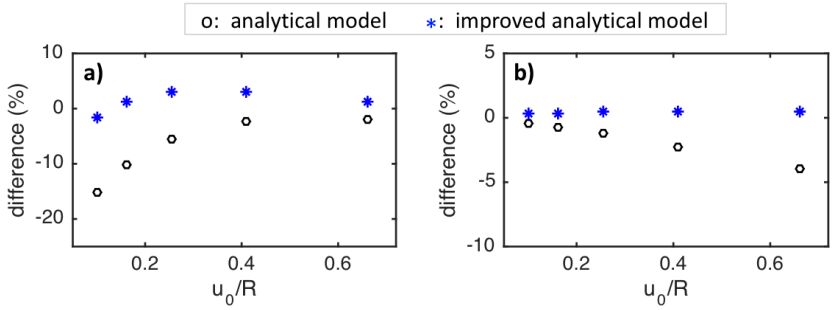

Figure 9. The differences between (a) the amplitudes of oscillations (here for the fifth peak) and (b) the steady-state displacements predicted by the analytical model (Eq. 1) and the improved analytical model (Eq. 13) and the finite element model for different force levels or dimensionless displacements ($G = 650$ Pa, $\rho = 1000$ kg/m^3, $\nu = 0.45$, $R = 0.5$ mm and ρ_s = 8000 kg/m^3).

The displacements of the sphere at an elastic medium interface for two other shear moduli precited by the analytical model (Eq. 1), the improved analytical model (Eq. 13) and the finite element model are shown in figure 10 ($f_0 = 0.8$ mN, $\rho = 1000$ kg/m^3, $\nu = 0.45$, $R = 0.5$ mm and ρ_s = 8000 kg/m^3). It is seen that, opposite to the original analytical model in [10], the results predicted by the improved analytical in this study and the finite element model are almost the same, as similar to the results obtained before for G = 650 Pa.

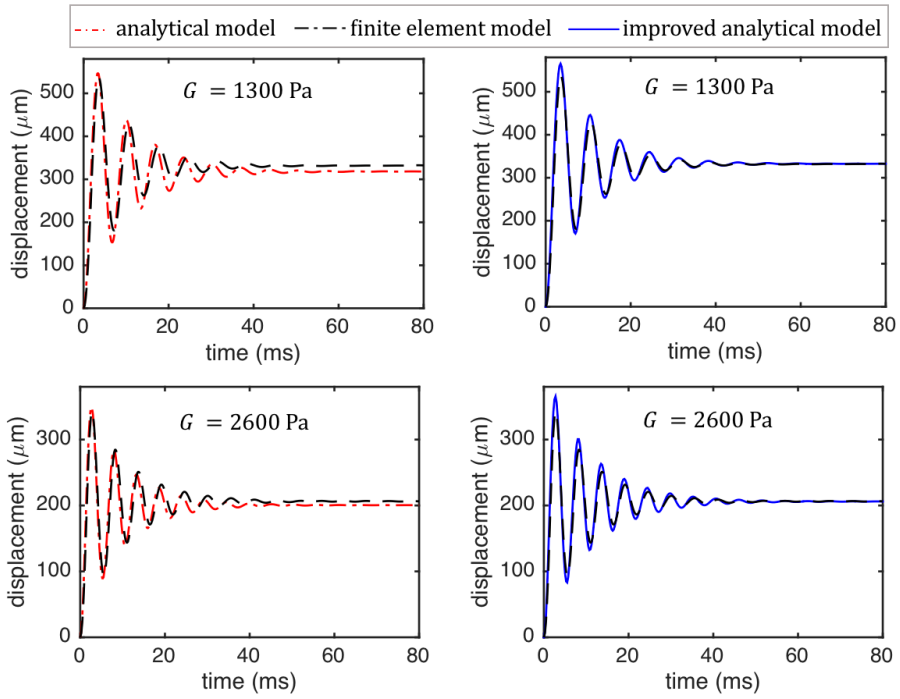

Figure 10. The displacements of the sphere at an elastic medium interface for two other shear moduli precited by the analytical model (Eq. 1), the improved analytical model (Eq. 13) and the finite element model ($f_0 = 0.8$ mN, $\rho = 1000$ kg/m^3, $v = 0.45$, $R = 0.5$ mm and $\rho_s = 8000$ kg/m^3).

The displacements of the sphere at an elastic medium interface for three different sphere density values are shown in figure 11 ($f_0 = 1.0$ mN, $G = 2600$ Pa, $\rho = 1000$ kg/m^3, $v = 0.45$ and $R = 0.5$ mm). It is again seen the amplitudes and frequencies or periods of oscillations and the steady-state displacements predicted by the improved analytical model (Eq. 13) and the finite element model are close to each other, though there are some differences between the analytical model (Eq. 1) and the finite element analysis results. The results show that the period of oscillations increases or the frequency of oscillations decreases with the increasing sphere density as expected (see Eqs. 16 and 18). It should be noted that the effective damping of the system decreases with the increasing sphere density (see Eqs. 16 and 20). Therefore, as seen in figure 11, the amplitudes of oscillations decrease as the sphere density increases. On the other hand, the steady-state displacement does not change with sphere density as expected.

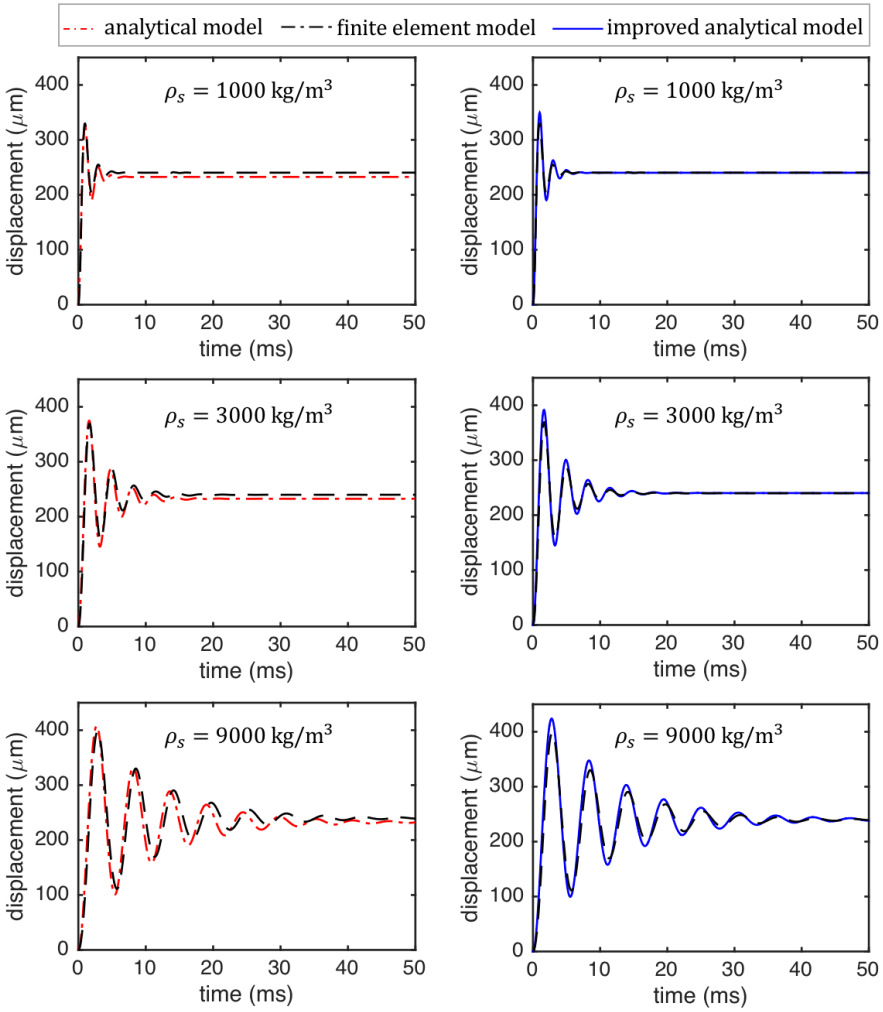

Figure 11. The displacements of the sphere at an elastic medium interface for three different sphere density values ($f_0 = 1.0$ mN, $G = 2600$ Pa, $\rho = 1000$ kg/m^3, $v = 0.45$ and $R = 0.5$ mm).

In addition to the soft elastic medium properties used so far, the displacements of the sphere at an elastic medium interface for three different higher shear moduli (0.1 – 10 GPa) predicted by the analytical model (Eq. 1), the improved analytical model (Eq. 13) and the finite element model are shown in figure 12 ($\rho = 1000$ kg/m^3, $v = 0.45$, $R = 0.5$ mm and ρ_s = 9000 kg/m^3). As seen the period of oscillations decreases (or the frequency of oscillations increases) as the shear modulus of the medium increases as expected. Opposite to the original analytical model in [10], the results predicted by the improved analytical in this study and the finite element model are almost the same for all shear modulus values. The model presented here can be used for both soft and stiff medium materials.

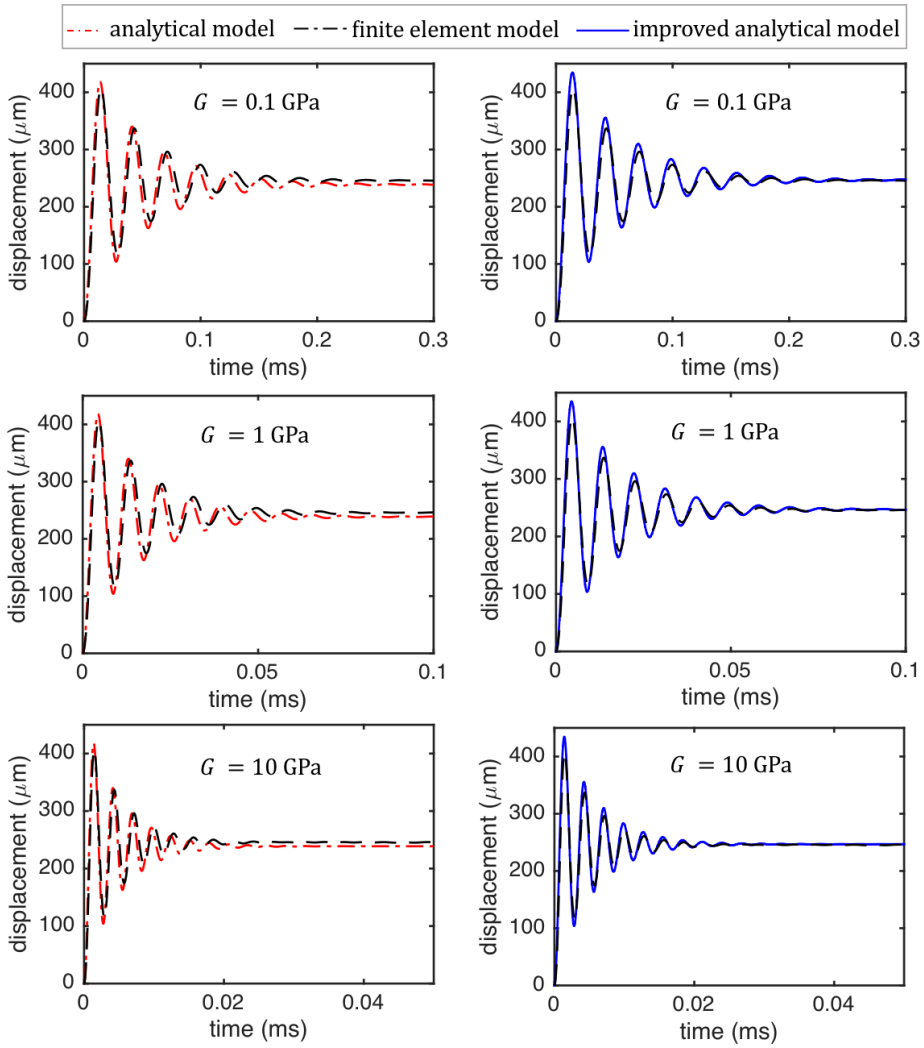

Figure 12. The displacements of the sphere at an elastic medium interface for three different shear moduli predicted by the analytical model (Eq. 1), the improved analytical model (Eq. 13) and the finite element model ($\rho = 1000$ kg/m^3, $\nu = 0.45$, $R = 0.5$ mm and $\rho_s = 9000$ kg/m^3 and $f_0 = 40, 400$ and 4000 N for the medium with 0.1, 1 and 10 GPa, respectively).

The developed model in this study can be used to understand the dynamic responses of spherical objects at medium interfaces in practical applications. Furthermore, the developed model is a remarkable tool for undergraduate and graduate students and researchers in the fields of engineering, materials science and physics to gain insight into the dynamic responses of spheres at medium interfaces. The students can exploit this study to use the finite element method to model the sphere at an elastic medium interface (Section 2.2) or any other system. This study can be referred for gaining insight into the reflections from the boundaries (figure 3), understanding the radiation damping, deriving the equation of motion of the sphere at a medium interface or similar systems, and obtaining an analytical solution for a damped system (Section 3).

4. Conclusion

In this study, an analytical model for predicting the small and large displacements of the sphere on an elastic half-space exposed to a dynamic force is developed. In addition to considering the elastic properties of the medium and the size of the sphere, the model developed in this study takes into account the density of the medium, the mass of the sphere and the radiation damping for dynamic loading. The results show that the amplitudes and frequencies of oscillations and the steady-state displacements precited by the proposed model are very close to the finite element analysis results. The proposed model can be used to understand the dynamic responses of spheres at medium interfaces in practical applications. Furthermore, the developed model can be a remarkable tool for undergraduate and graduate students in the fields of engineering, materials science and physics to understand how to derive the equation of motion of the sphere at a medium interface by considering radiation damping, to obtain an analytical solution for a damped system, and to use the finite element method to investigate the same problem.

ORCID

Hasan Koruk: https://orcid.org/0000-0003-4189-6678

References

[1] Kontomaris S V and Stylianou A 2017 Atomic force microscopy for university students: applications in biomaterials *Eur. J. Phys.* **38** 33003
[2] Binnig G, Quate C F and Gerber C 1986 Atomic force microscope *Phys. Rev. Lett.* **56** 930–3
[3] Kontomaris S V, Stylianou A, Nikita K S and Malamou A 2019 Determination of the linear elastic regime in AFM nanoindentation experiments on cells *Mater. Res. Express* **6** 115410
[4] Chang Y-R, Raghunathan V K, Garland S P, Morgan J T, Russell P and Murphy C J 2014 Automated AFM force curve analysis for determining elastic modulus of biomaterials and biological samples. *J. Mech. Behav. Biomed. Mater.* **37** 209–18
[5] Heim A J, Matthews W G and Koob T J 2006 Determination of the elastic modulus of native collagen fibrils via radial indentation *Appl. Phys. Lett.* **89** 181902
[6] Johnson K L 1985 *Contact Mechanics* (Cambridge University Press)
[7] Kontomaris S V and Malamou A 2021 A novel approximate method to calculate the force applied on an elastic half space by a rigid sphere *Eur. J. Phys.* **42** 25010
[8] Kontomaris S-V and Malamou A 2020 Small oscillations of a rigid sphere on an elastic half space: a theoretical analysis *Eur. J. Phys.* **41** 55004
[9] Kontomaris S-V and Malamou A 2021 Exploring the non-linear oscillation of a rigid sphere on an elastic half-space *Eur. J. Phys.* **42** 25011
[10] Koruk H 2021 Development of a model for predicting dynamic response of a sphere at viscoelastic interface: A dynamic Hertz model *IOP Conf. Ser. Mater. Sci. Eng.*
[11] Aglyamov S R, Karpiouk A B, Ilinskii Y A, Zabolotskaya E A and Emelianov S Y 2007 Motion of a solid sphere in a viscoelastic medium in response to applied acoustic

radiation force: Theoretical analysis and experimental verification *J. Acoust. Soc. Am.* **122** 1927–36
[12] Koruk H and Choi J J 2018 Displacement of a bubble by acoustic radiation force into a fluid-tissue interface *J. Acoust. Soc. Am.* **143**
[13] Koruk H and Choi J J 2019 Displacement of a bubble located at a fluid-viscoelastic medium interface *J. Acoust. Soc. Am.* **145** EL410-EL416
[14] Koruk H 2021 Assessment of the models for predicting the responses of spherical objects in viscoelastic mediums and at viscoelastic interfaces *IOP Conf. Ser. Mater. Sci. Eng.*
[15] Koruk H, El Ghamrawy A, Pouliopoulos A N and Choi J J 2015 Acoustic particle palpation for measuring tissue elasticity *Appl. Phys. Lett.* **107**
[16] Bezer J H, Koruk H, Rowlands C J and Choi J J 2020 Elastic deformation of soft tissue-mimicking materials using a single microbubble and acoustic radiation force *Ultrasound Med. Biol.* **46** 3327–38
[17] Kaster T, Sack I and Samani A 2011 Measurement of the hyperelastic properties of ex vivo brain tissue slices *J. Biomech.* **44** 1158–63
[18] Liu Y-L, Liu D, Xu L, Su C, Li G-Y, Qian L-X and Cao Y 2018 In vivo and ex vivo elastic properties of brain tissues measured with ultrasound elastography *J. Mech. Behav. Biomed. Mater.* **83** 120–5
[19] Chen E J, Novakofski J, Jenkins W K and O'Brien W D 1996 Young's modulus measurements of soft tissues with application to elasticity imaging *IEEE Trans. Ultrason. Ferroelectr. Freq. Control* **43** 191–4
[20] Koruk H, Dreyer J T and Singh R 2014 Modal analysis of thin cylindrical shells with cardboard liners and estimation of loss factors *Mech. Syst. Signal Process.* **45** 346–59
[21] D.J. Inman 1994 *Engineering Vibration* (Englewood Cliffs, New Jersey: Prentice-Hall International, Inc.)